Maximizing Kinematic Motion for a 3-DOF VGT Module

Robert L. Williams II
Eric R. Hexter
Ohio University
Athens, OH 45701

Journal of Mechanical Design
Transactions of the ASME
Vol. 120, No. 2, 1998, pp. 333-336

Contact author information:
Robert L. Williams II
Assistant Professor
Department of Mechanical Engineering
257 Stocker Center
Ohio University
Athens, OH 45701-2979
Phone: (740) 593-1096
Fax: (740) 593-0476
E-mail: bobw@bobcat.ent.ohiou.edu

Maximizing Kinematic Motion for a 3-DOF VGT Module

R. L. Williams II and E. R. Hexter

This article presents design results for maximizing kinematic motion range in three-degree-of-freedom (DOF) double-octahedral variable-geometry-truss (VGT) modules modeled as extensible gimbals. Design curves are presented to describe motion and results are summarized.

1 Introduction

The double-octahedral variable geometry truss (VGT) module was developed by NASA for use in deployable space structures (Rhodes and Mikulas, 1985). It has also been proposed for use as joints in hyper-redundant, long-reach manipulators (Chen and Wada 1990; Hughes et.al., 1991; Salerno and Reinholtz, 1994). Authors (e.g. Chirikjian and Burdick, 1991; Salerno and Reinholtz 1994; Williams and Mayhew, 1996) have developed methods for controlling such manipulators. The potential advantages of VGT manipulators are well known. A major disadvantage of VGTs is limited range of motion compared to serial manipulators.

Padmanabhan, et.al. (1992a) proposed position control of a single VGT module by modeling the complex in-parallel-actuated kinematics by a simpler virtual serial extensible gimbal model. This idea was extended to position control of two VGT modules by Padmanabhan et.al. (1992b) and later implemented in position and rate at NASA (Williams et.al., 1995). This article presents a study using kinematic design curves to maximize motion for this module.

2 Double Octahedral VGT Module

The kinematic diagram is shown in Fig. 1. As a joint in a VGT-based manipulator, it is convenient to control the VGT as an extensible gimbal (Padmanabhan et.al., 1992a). Figure 2 shows the virtual extensible gimbal kinematic diagram. The inputs are L_1, L_2, L_3 and the outputs are gimbal angles α, β about mutually perpendicular axes and *r*, a symmetric accordion-like variable which extends or contracts the length of the joint.

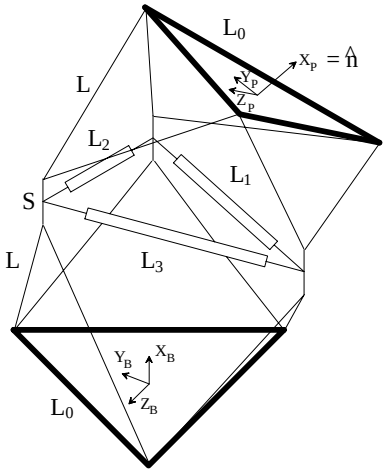

Figure 1.
VGT Module Diagram

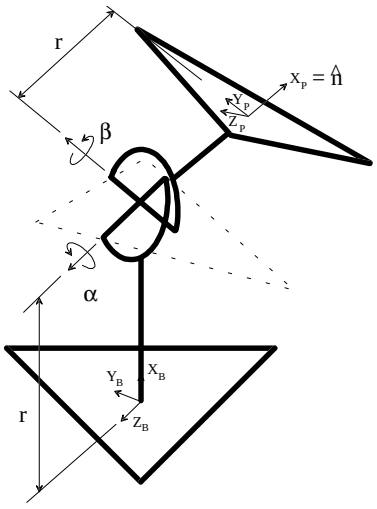

Figure 2.
Extensible Gimbal Diagram

The VGT possesses a high degree of symmetry, as shown in Fig. 1. The top and bottom planes are equilateral triangles with batten length L_0. The middle plane consists of identical actuators with variable lengths L_1, L_2, L_3 with limits $L_{\min}$ and $L_{\max}$. Two stages of six longerons of length *L* connect the bottom, middle, and top planes. In an ideal VGT module, six struts connect via five spherical joints at each midplane vertex. This is difficult to achieve in practice so an offset *S* is included in the model. Five constant parameters are required to define the VGT. We will normalize by *L* so there are four independent dimensionless parameters:

$$\frac{L_0}{L} \qquad \frac{L_{\min}}{L} \qquad \frac{L_{\max}}{L_{\min}} \qquad \frac{S}{L}$$

L=1 is used since α, β will not change given the above parameters and r results scale by L. $L_{\max}$ is related to $L_{\min}$ instead of L to facilitate linear actuator specification.

The automatic generation of kinematic design curves for the VGT module requires repeated inverse position kinematics solutions. Padmanabhan et.al. (1992a) first presented this solution for the VGT module. Detailed VGT forward and inverse position kinematic solutions are presented by Williams (1994), based on the work of Padmanabhan et.al. (1992a).

The inverse kinematics solution calculates the actuator lengths L_1, L_2, L_3 given the desired gimbal outputs α, β, r. The top plane is symmetric to the fixed bottom plane, mirrored about the mid-plane for all L_1, L_2, L_3. This condition enables a straight-forward, closed-form inverse kinematics solution.

3 Generation of Kinematic Design Curves

VGT module kinematic design curves were generated automatically by computer, using the inverse kinematics solution over the four-dimensional design parameter space. This article assumes several 3-DOF VGT modules will be used to form a long-reach manipulator. In such a manipulator, the α, β range is crucial in maximizing overall workspace and r is less important. Therefore, the extreme α, β angles are maximized in this article. Though r plays a crucial role in maximizing α, β, its range of motion is not maximized For each design parameter set, the gimbal extension r (normalized by L) was varied from r_{min}/L to r_{max}/L in small increments (r_{min}/L and r_{max}/L vary for each case) to find the extreme α, β. For each four-parameter set, β is set to zero, r is fixed and α is increased until the inverse kinematics solution determines one or more $L_{\min}$, $L_{\max}$ joint limits are violated. Maximum negative

α is then found similarly. The extension output r is incremented to find the next extreme α angles. Angle β extremes are found in the same manner, with α set to zero. For the VGT modules, an extreme gimbal angle occurs only when the second gimbal angle is held to zero. The constant parameter ranges are chosen to a cover reasonable design space, the center of which is motivated by NASA-built hardware (Rhodes and Mikulas, 1985):

$$\frac{L_0}{L}: \qquad 0.50 \le \frac{L_0}{L} \le 1.50 \text{, step } 0.04$$

$$\frac{L_{\min}}{L}: \qquad \frac{L_{\min}}{L} = 1, \frac{L_0}{L}, \frac{L_{avg}}{L} \qquad \left(L_{avg} = \frac{L + L_0}{2} \right)$$

$$\frac{L_{\max}}{L_{\min}}: \qquad \frac{L_{\max}}{L_{\min}} = 1.25, 1.50, 1.75$$

$$\frac{S}{L}: \qquad \frac{S}{L} = 0, 0.05, 0.10, 0.15$$

Three-dimensional plots of extreme α vs. r/L vs. L_0/L and β vs. r/L vs. L_0/L were generated. Thirty-six α and thirty-six β design charts were created, spanning the design space (4 S/L values x 3 $L_{\max}/L_{\min}$ values x 3 $L_{\min}/L$ values).

4 Results

Figures 3 and 4 show the extreme α, β angles versus the normalized gimbal extension r/L, for (non-optimal) parameters $L_0/L = 1.06$, $L_{\min}/L = L_{avg}/L$, $L_{\max}/L_{\min} = 1.75$, and $S/L = 0.05$. The upper curves define the maximum positive and the lower the maximum negative gimbal angles. All values in between the curves are feasible for the extensible gimbal. At the minimum and maximum r/L values (here, 0.45 and 0.81) zero gimbal angle motion is possible. The β case is symmetric while the α case is not. This means that the maximum positive α occurs at a different r/L value than the maximum

negative α. Note that the maximum positive α value is extremely sensitive to small changes in *r*/*L* near the upper end of the gimbal extension. Due to module symmetry, one would expect both α and β symmetry. However, the α axis is not an axis of symmetry for the mid-plane, as evident in Figure 2.

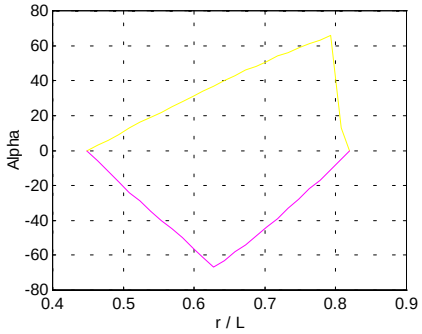

Figure 3.
Maximum α vs. Extension

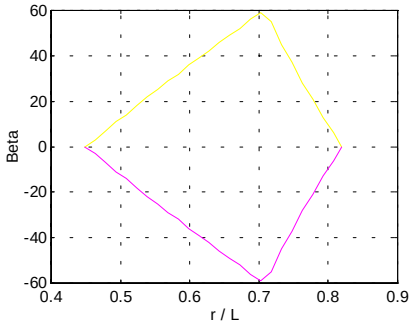

Figure 4.
Maximum β vs. Extension

For the four-dimensional design parameter space, the maximum α, β, and r/L all occur at the same values: $L_0/L = 1.14$, $L_{\min}/L = L_{avg}/L$, $L_{\max}/L_{\min} = 1.75$, and $S/L = 0$. Figures 5 and 6 present the extreme (maximum of the maximum angles for all thirty-six cases) α, β results. From Figs. 5 and 6 it is seen that planar plots similar to Figs. 3 and 4 are translated along a curving spine. Figs. 5c and 6c show where the maximum/minimum α, β values occur: the maximum positive α values ('x' in Fig. 5c) occur close to r_{max} in each case (as Fig. 3 also shows); the maximum negative α values ('o' in Fig. 5c) occur closer to the middle of the *r* range; the maximum positive and negative β values occur at the same *r* value in each case ('o' in Fig. 6c).

The extreme α values $73^\circ, -75^\circ$ in Fig. 5 occur for different r/L values. The extreme β values $\pm 68^\circ$ in Fig. 6 occur for the same r/L value. The extreme r/L range (0.33,0.77) also occurs in the module with the extreme α, β. Figures 5 and 6 show results up to the extreme cases $L_0/L = 1.14$ for

clarity. As L_0 / L increases from that optimal value, the maximum α, β values and r / L range decrease, in similar (shrinking) planar shapes curving along the spine.

The kinematically-optimal VGT module corresponding to Figs. 5 and 6 is shown in Fig. 7, with all actuators set to mid-length. For comparison, one of the remaining thirty-five non-optimal cases is shown in Fig. 8, with $L_0 / L = 0.50$, $L_{\min} / L = 1$, $L_{\max} / L_{\min} = 1.50$, and $S / L = 0.10$. In Fig. 8, the maximum outputs are: α 50°,–40°, β ±38°, and r / L (0.65,0.87), which are much lower than those of Fig. 7.

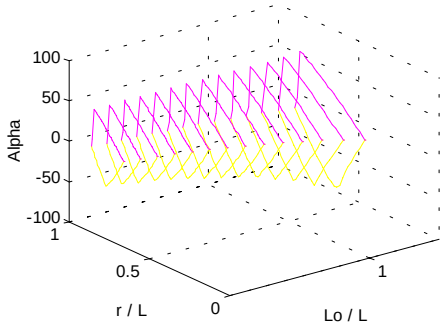

Figure 5a. Extreme α Case

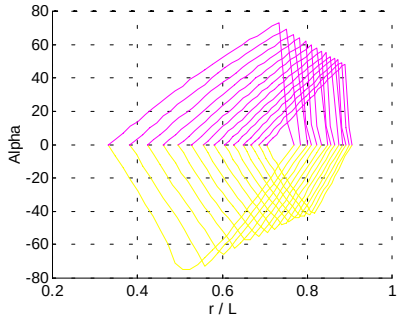

Figure 5b. α Right-Side View

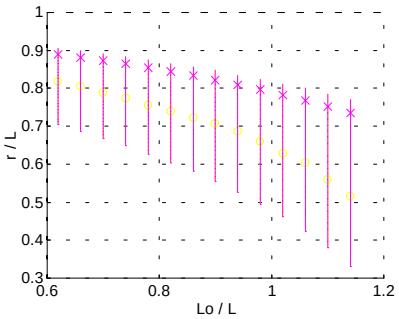

Figure 5c. α Top View

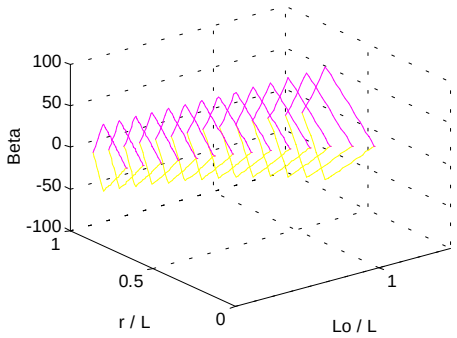

Figure 6a. Extreme β Case

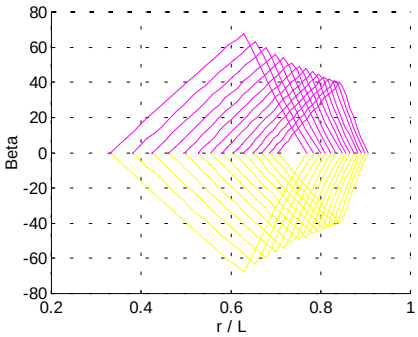

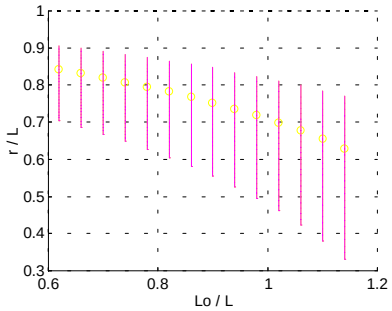

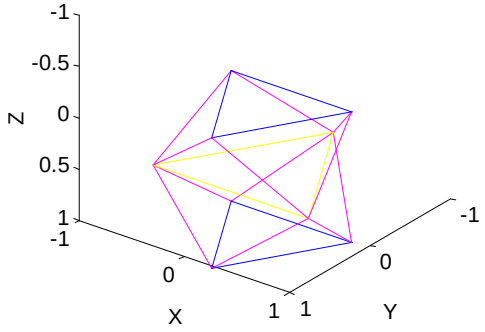

Figure 7. Optimal VGT

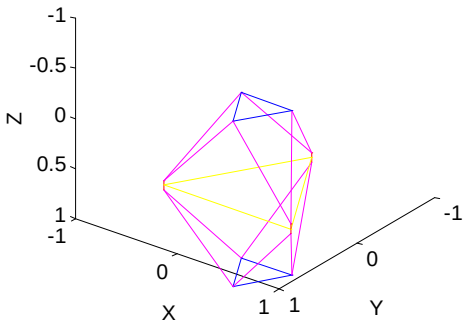

Figure 8. Non-optimal VGT

The design parameter which has the greatest effect was the L_{max} / L_{min} ratio. Obviously, the greatest kinematic motion range results with the greatest possible L_{max} / L_{min} ratio. The next important

parameter is $L_{\min}$. The optimal value for $L_{\min}/L$ is L_{avg}/L and the optimal L_0/L is 1.14. The normalized joint offset parameter S/L had a minimal effect on the articulation angles, but it did affect the location of r/L values for maximum gimbal angles. However, $\Delta r/L$ is not affected by *S*. The insensitivity of output parameters to *S* is good for practical VGT design because it is difficult to fabricate joints without an offset. However, zero joint offset is preferable because it leads to the highest outputs (only marginally higher than optimal cases with finite offset) and structural characteristics are improved with zero joint offset.

Table 1 summarizes the maximum results for all design parameter sets considered in this article. Angle units are degrees and lengths are dimensionless in Table 1. Since the joint offset parameter S/L has minimal effect on the maximum output values $\alpha, \beta, r/L$, only nine of the thirty-six cases are reported. All nine cases in Table 1 have design parameter $S/L = 0$. Cases 10-18 ($S/L = 0.05$), 19-27 ($S/L = 0.10$), and 28-36 ($S/L = 0.15$) are not reported because the results are similar to Table 1.

Table 1. Maximum VGT Kinematic Output Summary

Case	L_{max}/L_{min}	L_{min}/L	α	β	r/L	$\Delta r/L$	L_0/L
1	1.25	1	22,-19	± 17	0.78,0.87	0.09	0.50
2	1.25	L_0/L	41,-53	± 38	0.26,0.54	0.28	1.46
3	1.25	L_{avg}/L	21,-25	± 20	0.47,0.60	0.13	1.50
4	1.50	1	50,-40	± 38	0.65,0.87	0.22	0.50
5	1.50	L_0/L	57,-61	± 50	0.36,0.69	0.33	1.22
6	1.50	L_{avg}/L	53,-73	± 53	0.30,0.63	0.33	1.42
7	1.75	1	67,-73	± 58	0.49,0.85	0.36	0.78
8	1.75	L_0/L	72,-74	± 65	0.37,0.78	0.41	1.06
9	1.75	L_{avg}/L	73,-75	± 68	0.33,0.77	0.44	1.14

The extreme case of Figs. 5, 6, and 7 is given in case 9 of Table 1. This is the absolute maximum result, although cases 18, 27, and 36 are close because the increasing S / L offset parameter has little effect. The non-optimal module pictured in Fig. 8 is case 22 (similar to case 4).

5 Conclusion

This article gives a basis for maximizing kinematic motion in three-DOF double-octahedral VGT modules modeled as extensible gimbals. In-parallel-actuated manipulators generally suffer from restricted kinematic motion ranges and thus should be designed to achieve the maximum possible motion. The joint offset parameter was found to have little effect on the output parameters. Only symmetric modules were considered since manipulators should be general-purpose. Parameters for the optimal module are reported subject to the range of parameters considered. The design curves relate how the maximum outputs change for different parameter values. Virtual gimbal angle limits are configuration-dependent since they depend on virtual gimbal extension.

6 References

Chen, G.S., and Wada, B.K., 1990, “On an Adaptive Truss Manipulator Space Crane Concept”, *1st Joint US/Japan Conference on Adaptive Structures*, Maui, Hawaii, pp. 726-742.

Chirikjian, G.S., and Burdick, J.W., 1991, "Parallel Formulation of the Inverse Kinematics of Modular Hyper-Redundant Manipulators", *1991 IEEE International Conference on Robotics and Automation*, Sacramento, CA, pp. 708-713.

Hughes, P.C., Sincarsin, W.G., and Carroll, K.A., 1991, “Trussarm: A Variable Geometry Truss Manipulator”, Journal of Intelligent Materials, Systems, and Structures, Vol. 2, pp.148-161.

Padmanabhan, B., Tidwell, P.H., Salerno, R.J., and Reinholtz, C.F., 1992a, "VGT-Based Gimbals: Practical Construction and General Theory", *1992 ASME Mechanisms Conference,* DE-Vol. 47, Phoenix, AZ, pp. 437-443.

Padmanabhan, B., Arun, V., and Reinholtz, C.F., 1992b, “Closed-Form Inverse Kinematic Analysis of Variable-Geometry Truss Manipulators”, **Journal of Mechanical Design**, Vol. 114, September, pp. 438-443.

Rhodes, M.D., and Mikulas, M.M., Jr., 1985, "Deployable Controllable Geometry Truss Beam", *NASA Technical Memorandum 86366.*

Salerno, R.J., and Reinholtz, C.F., 1994, "A Modular, Long-Reach, Truss-Type Manipulator for Waste Storage tank Remediation", *1994 ASME Mechanisms Conference*, DE-Vol. 72, Minneapolis, MN, September, pp. 153-159.

Williams, R.L., II, and Mayhew, J.B., IV, 1996, "Control of Truss-Based Manipulators using Virtual Serial Models", *1996 ASME Design Technical Conferences, 24th Biennial Mechanisms Conference*, Irvine, CA, August.

Williams, R.L., II, Horner, C.G., and Remus, R.G., 1995, "Control of a Variable Geometry Truss Module as an Extensible Gimbal", *ANS Sixth Topical Meeting on Robotics and Remote Systems*, Monterey, CA, February**.**

Williams, R.L., II, 1994, "Kinematic Modeling of a Double Octahedral Variable Geometry Truss (VGT) as an Extensible Gimbal", *NASA Technical Memorandum 109127*, NASA Langley Research Center, Hampton, VA**.**